Carbohydrate Polymers 99 (2014) 432–437

Contents lists available at ScienceDirect

Carbohydrate Polymers

journal homepage: www.elsevier.com/locate/carbpol

Conformation and physical properties of cycloisomaltooligosaccharides in aqueous solution

Shiho Suzuki [a], Takashi Yukiyama [a], Arata Ishikawa [a], Yoshiaki Yuguchi [b], Kazumi Funane [c], Shinichi Kitamura [a,*]

[a] Graduate School of Life and Environmental Sciences, Osaka Prefecture University, Sakai 599-8531, Japan
[b] Faculty of Engineering, Osaka Electro-Communication University, Neyagawa, Osaka 572-8530, Japan
[c] Applied Microbiology Division, National Food Research Institute, National Agriculture and Food Research Organization, 2-1-12 Kannondai, Tsukuba 305-8642, Japan

ARTICLE INFO

Article history:
Received 16 May 2013
Received in revised form 18 July 2013
Accepted 26 July 2013
Available online 22 August 2013

Keywords:
Cycloisomaltooligosaccharide
Intrinsic viscosities
Small angle X-ray scattering
Molecular dynamic simulation

ABSTRACT

We studied the conformation and physical properties of cyclic and linear isomaltooligosaccharides in aqueous solution by intrinsic viscosity measurement, small angle X-ray scattering (SAXS) and molecular modeling. We used four cycloisomaltooligosaccharide samples (CIs) with degree of polymerization (DP) 7–10 (CI-7–CI-10) and five linear isomaltooligosaccharide samples (LIs) with DP 7–11 (LI-7–LI-11). The values of α in the Mark–Houwink–Sakurada equation $[\eta] = KM_w^{\alpha}$ for the CI and LI were determined to be 0.50 and 0.78, respectively. The radii of gyration (R_G) of CI-7, CI-8, CI-9 and CI-10 determined from SAXS data were 6.7, 6.9, 7.5 and 8.3 Å, respectively. The scattering profile of CI-9 compared with those obtained for molecular models indicated that CI molecular chains are less flexible than those for LIs and adopt a rather compact circular conformation.

1. Introduction

Among cyclooligosaccharides, cyclodextrins, which are composed of α-(1→4)-linked D-glucopyranose units, have been studied and used industrially for many purposes. A large number of cyclic oligo- and polysaccharides have also been discovered (Kitamura, 2002). Among these, cycloisomaltooligosaccharides (cyclodextrans) are of interest since these cyclic glucans have the same repeating unit as cyclodextrins, glucose, but different glycosidic linkages: α-(1→6) linkages.

Cycloisomaltooligosaccharides (designated CI in this study) are produced from dextran catalyzed by cycloisomaltooligosaccharide glucanotransferase (CITase, EC 2.4.1.248) (Oguma, Tobe, & Kobayashi, 1994). CIs with degree of polymerization (DP) ranging from 7 to 17 have been found (Funane et al., 2008; Oguma, Horiuchi, & Kobayashi, 1993). Some functional properties of CIs have been reported: high solubility in water, inhibition of the dextransucrase reaction (Kobayashi, Funane, & Oguma, 1995) and complex formation of CI-10 with Victoria blue B (Funane et al., 2007). However, the conformation of CIs in solution is unknown.

In this study, we describe the conformation and physical properties of linear and cycloisomaltooligosaccharides in aqueous solution using intrinsic viscosity measurement, small angle X-ray scattering (SAXS) and molecular modeling.

2. Experimental

2.1. Materials

Four CI samples with DP 7–10 (CI-7–CI-10) were fractionated from a cycloisomaltooligosaccharide mixture produced from dextran by the action of cycloisomaltooligosaccharide glucanotransferase (CITase, EC 2.4.1.248) as described previously (Funane et al., 2008). The CI samples were fractionated by reversed-phase chromatography using an ODS column (Daisopak SP-120-5-ODS-BP, 20 i.d. × 250 mm, Daiso, Osaka, Japan). The HPLC pump used was LC-6AD (Shimadzu, Kyoto, Japan). The flow rate was 10 mL/min. CI-7, CI-8 and CI-9 were eluted with 7% (v/v) methanol and CI-10 was eluted with 9% (v/v) methanol. The peaks for each CI were detected by a refractive index detector (Shodex RI-71, Showa Denko K.K., Tokyo, Japan). Samples were collected, concentrated and then lyophilized.

Five LI samples with degree of polymerization (DP) 7–11 (LI-7–LI-11) were fractionated from dextran hydrolyzate which was prepared by hydrolyzation of Dextran T-10 (Pharmacia, Sweden) in 0.1 N HCl at 100 °C for 1 h. The hydrolyzate was size fractionated by gel permeation chromatography using a Toyopearl HW-40S column (5 i.d. × 62 cm, Tosoh Corporation, Japan) with a flow rate of

* Corresponding author. Tel.: +81 72 254 9457; fax: +81 72 254 9458.
E-mail address: skita@bioinfo.osakafu-u.ac.jp (S. Kitamura).

0144-8617/$ – see front matter © 2013 Elsevier Ltd. All rights reserved.
http://dx.doi.org/10.1016/j.carbpol.2013.07.089

2 mL/min. The fractions containing LIs with DP 5–11 were collected. The size-fractionated LI mixtures were loaded onto an ODS column and eluted with 6% (v/v) methanol using the same HPLC system used for preparation of cyclic samples. These isolated samples for each LI were collected, concentrated, and lyophilized.

Fractionated CI and LI samples were analyzed by high-performance anion-exchange chromatography using a pulsed amperometric detector (HPAEC–PAD) system with a CarboPac PA100 column (4 i.d. × 250 mm, Dionex, CA). A Dionex ICS-3000 HPAEC system (Dionex, MA) with a PAD detector was used.

We measured proton NMR spectra of CI-9 and LI-9 at 80 °C in D_2O using a JNM-AL400 spectrometer (JEOL Ltd., Tokyo, Japan). Before NMR measurement, all exchangeable H in the samples was replaced by D in deuterium oxide. The sample concentration was 5 mg/mL. DSS (4,4-dimethyl-4-silapentane-1-sulfonic acid) (δ_H = 0.00 ppm) was used as the internal standard for the chemical shift.

We analyzed the linkage pattern of CI-9 and LI-9 by methylation analysis according to a previously reported method (Maeda, Zhu, Suzuki, Suzuki, & Kitamura, 2004).

2.2. TOF-MS

The molecular mass of CIs and LIs was measured by matrix-assisted laser-desorption time of flight spectroscopy (MALD-TOF). The samples were dissolved in 10% methanol solution containing 100 mM 2,5-dihydroxybenzoic acid. 2 μL of this mixture was applied to a MALD probe and dried. MALD-TOF spectra were recorded with a Bruker Daltonics autoflex II spectrometer (Bruker Daltonics Inc., MA).

2.3. Intrinsic viscosity measurement

The intrinsic viscosities [η] of CI and LI in aqueous solution at 25 ± 0.020 °C were determined using an Ubbelohde-type viscometer having a flow-through time about 180 sec for the solvent. The concentrations of the sample solutions were 8.0, 10.0, 13.3, 16.0 and 20.0 mg/mL. The sample solution and solvent were filtered with a 0.45 μm membrane filter. The sample solution was diluted by adding solvent by pipette directly to the viscometer. The dynamic energy was not corrected. [η] was obtained at zero concentration by extrapolation of the plots of reduced viscosity against concentration.

2.4. Small-angle X-ray scattering (SAXS)

We measured small-angle X-ray scattering (SAXS) of CIs and LIs in aqueous solutions at four concentrations at 25 °C. The SAXS experiments were performed at BL40B2 in SPring-8, Hyogo, Japan. The wavelength (λ) of the incident X-ray beam was adjusted to 0.1 nm. A flat sample cell of 3 mm in path-length was made of stainless steel with quartz windows of 20 μm thickness. The scattered X-ray was detected with an imaging plate (IP). The obtained two-dimensional data was transformed to one-dimensional data by circular averaging. The excess scattering intensities were calculated by subtracting the scattering intensity of water.

The excess scattering intensity $I(q)$ was evaluated by subtracting the scattering intensity of the solvent from that of the solution. The $I(q)$ at small scattering angles can be approximated according to Guinier (Porod, 1982) as

$$I(q) \propto \exp\left(\frac{-R_G^2 \cdot q^2}{3}\right) \quad (1)$$

with a single parameter R_G defined as the radius of gyration of the solute molecule, where $q = (4\pi/\lambda)\sin(\theta/2)$ is the magnitude of the scattering vector and θ represents the scattering angle.

2.5. Molecular modeling and simulations

We produced several structures of CI-9 by dynamical simulated annealing at 373 K starting with chains having the desired glycosidic linkage torsion angles for (1 → 6)-glycosidic linkages, using the method of a previous report (Liu, Brant, Kitamura, Kajiwara, & Mimura, 1999).

Molecular dynamics simulations were carried out using the Discovery Studio Simulation module (Ver. 2.5, Accelrys Inc., CA). Calculations were performed using the CHARMm Force-Fields 35 b-1 (Brooks et al., 2009), as implemented in Discovery Studio. We take into account the solvation effect using the implicit solvent model of the generalized Born with simple switching (GBSW) method (Green, 2008; Im, Lee, & Brooks, 2003). GBSW solvation energies were computed using the GBSW routine within the CHARMm computer program. An internal solute dielectric of 1.0 was used, along with a solvent dielectric constant of 80.0.

As a result of annealing at 373 K, we obtained a structure having lower total energy (potential + kinetic energy). Starting from that structure, simulations were carried out with a time step of 1 fs at 300 K until the total energy was minimized after about 1100 ns. The production type was set NVT ensemble. The results between 1100 and 2300 ns were used to calculate the scattering function. Snapshots of the model were taken at 3 ns intervals.

The scattering profile $I(q)$ was calculated as a function of the magnitude of the scattering vector q from the atomic coordinates of the molecular model chains using the Debye formula (Glatter, 1980) according to a previously reported method (Kitamura et al., 1997; Liu et al., 1999; Mimura, Urakawa, Kajiwara, Kitamura, & Takeo, 1995; Shimada, Kaneko, Takada, Kitamura, & Kajiwara, 2000)

$$I(q) = \sum_{i=1}^{n} f_i^2 g_i^2(q) + 2\sum_{i=1}^{n-1}\sum_{j=i+1}^{n} f_i f_j g_i(q) \frac{\sin d_{ij} q}{d_{ij} q} \quad (2)$$

where f_i is an atomic scattering factor and d_{ij} is the distance between the ith and jth atoms. The form factor for a single atom $g_i(q)$ is assumed to be given by the form factor of a sphere which possesses a radius equivalent to the van der Waals radius of the ith atom as

$$g_i(q) = \frac{3[\sin(R_i q) - (R_i q)\cos(R_i q)]}{(R_i q)^3} \quad (3)$$

with R_i being the van der Waals radius of the ith atom. Only carbon and oxygen atoms are included in the sum in Eq. (2); the contribution of the hydrogen atoms to the X-ray scattering is ignored. The radii of carbon and oxygen atoms are taken to be 1.7 and 1.5 Å, respectively (Bondi, 1964; Goebel, Dimpfl, & Brant, 1970). The simulated scattering profiles were directly compared with those observed by SAXS by normalizing with respect to the scattered intensity at the zero angle.

Comparison of measured and theoretical $P(q)$ values was made in plots of $q^2P(q)$ vs. q (Kracky plot), since this plot is known to show marked differences between linear and cyclic species which are of the same physical dimensions (Burchard, 1986).

3. Results and discussions

3.1. Samples

We isolated four CI samples with DP of 7–10 (CI-7, CI-8, CI-9 and CI-10) from a CI mixture sample and five LI samples with DP of 7–11 (LI-7, LI-8, LI-9, LI-10 and LI-11) from an LI mixture sample. Each fractionated sample corresponds to a single peak in the HPAEC chromatogram (data not shown). The DP of the fractionated sample was determined by TOF-MS measurement. Fig. 1 shows TOF-MS spectra of CI-9 and LI-9 giving peaks at m/z 1482.4 $[M+Na]^+$ and

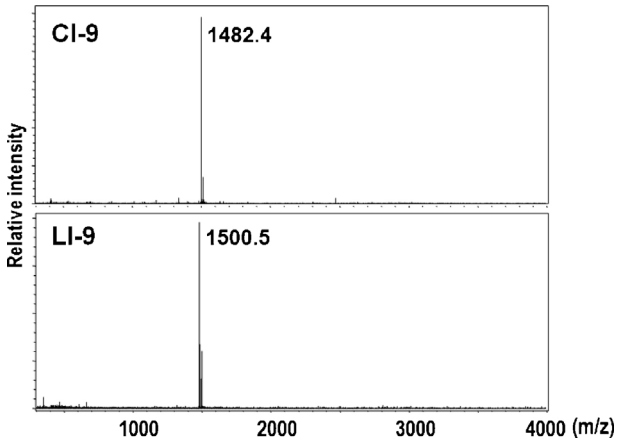

Fig. 1. TOF-MS spectra of CI-9 and LI-9.

m/z 1500.5 $[M+Na]^+$, respectively. This shows that the two samples are cyclic and linear nonasaccharides, respectively.

We measured the ^{1}H NMR spectra of all CIs and LIs (Fig. A.1). All CIs had similar spectra, as did all LIs. In the anomeric region of the spectra, all CI samples showed one signal at δ 4.93 ppm, whereas all LI samples showed three signals, one main signal at δ 4.93 ppm and two minor peaks at 4.62 and 5.21 ppm. The peak at 4.93 ppm was assigned to anomeric protons of → 6)-α-D-Glc*p*-(1 → residues and the peaks at 4.62 and 5.21 ppm were assigned to anomeric protons of reducing ends of the LIs. This indicates that CIs consist of only → 6)-α-D-Glc*p*-(1 → residues and have no reducing ends, and LIs consist of → 6)-α-D-Glc*p*-(1 → residues containing reducing ends. The spectra for the four CIs were essentially the same, as were those for the five LIs, so essentially there was one chemical structure for the CIs and another for the LIs. Consequently we used CI-9 and LI-9 for further analysis.

A sugar composition analysis of CI-9 and LI-9 showed that both oligosaccharides were composed of only glucose. We analyzed the glycosidic linkage of CI-9 by methylation analysis. In the GC–MS spectra of partially methylated alditol acetate derivatives of CI-9, CI-9 yielded one peak identified as 2,3,4-tri-*O*-methyl D-glucose. Thus CI-9 consists of only → 6)-α-D-Glc*p*-(1 → residues.

3.2. Intrinsic viscosities

The intrinsic viscosities are plotted against molecular weight (M) in Fig. 2. The intrinsic viscosity $[\eta]$ and Huggins constant k' for CI and LI samples are listed in Table A.1. The linear sample had higher intrinsic viscosity. The relation between the intrinsic viscosity and molecular weight is expressed by the Mark–Houwink–Sakurada equation $[\eta] = KM^{\alpha}$ (K and α are constants). From our data, we obtained the relations $[\eta] = 8.67 \times 10^{-2} M^{0.50}$ for CIs and $[\eta] = 1.39 \times 10^{-2} M^{0.78}$ for LIs. The values of α in the Mark–Houwink–Sakurada equation for the CI and LI were determined to be 0.50 and 0.78, respectively. The smaller α value reflects the ring shape of CI and means that the cyclic chains have more compact conformation than the linear one. This indicates that CI molecular chains have a rather compact circular conformation and may be less flexible than those for LIs, whereas LI chains are random coils solvated with water.

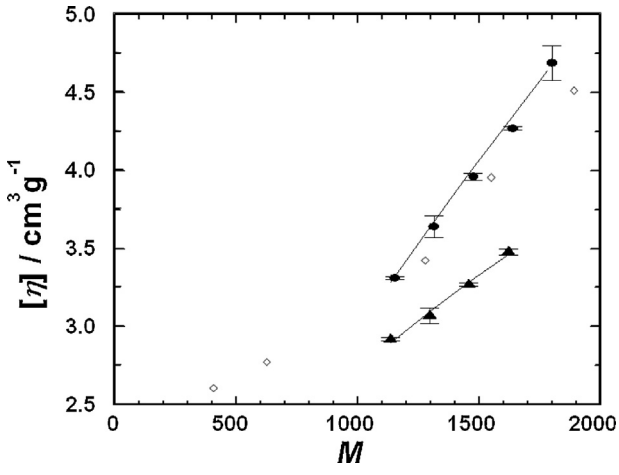

Fig. 2. Plots of $[\eta]$ vs. molecular weight for CIs (filled triangle) and LIs (filled circle), along with reported values for LIs (open diamond) (Gekko & Noguchi, 1971).

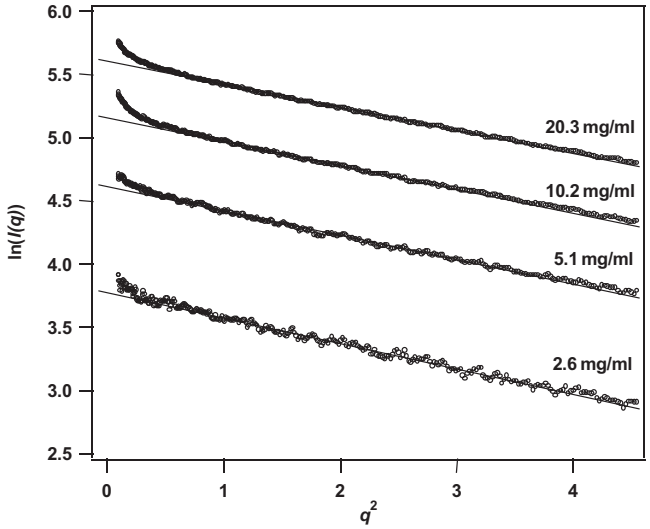

Fig. 3. Guinier plots of SAXS data for CI-9 in water at four concentrations.

Gekko et al. also measured the viscosity of linear isomaltooligosaccharides (Gekko & Noguchi, 1971). Their data were lower than our data (Fig. 2). This is probably because their samples were polydisperse and may have contained other DP samples, whereas our samples are monodisperse.

3.3. Small angle X-ray scattering

Fig. 3 shows the Guinier plots of SAXS data for CI-9. The radius of gyration (R_G) is not very dependent on concentration (Fig. 4). For example, the apparent R_G of CI-9 was estimated to be 7.7, 7.6, 7.5 and 7.4 Å for oligomer concentrations of 2.6, 5.1, 10.2 and 20.3 mg/mL, respectively. The R_G values at zero concentration were determined by linear extrapolation. Table 1 summarizes

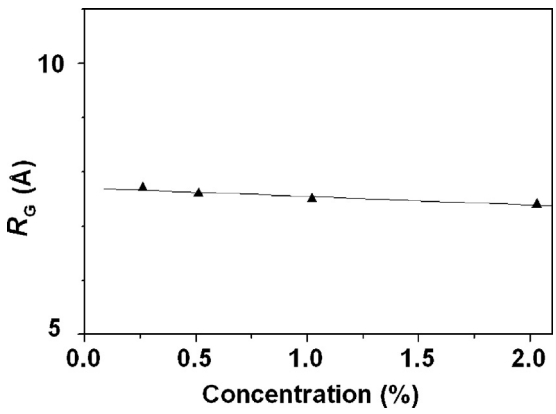

Fig. 4. Plots of R_G for CI-9 vs. concentration.

Table 1
The R_G values for CIs and LIs.

DP	R_G (Å)	
	CI	LI
7	6.7 (6.3[a])	7.8 (7.3[c])
8	6.9 (6.6[b])	8.3 (8.1[c])
9	7.5 (6.9[b])	9.2
10	8.3 (7.5[b])	9.8
11	–	10.1

Values in parentheses are the R_G values for cyclic and linear maltooligosaccharides.
[a] Shimada et al. (2000).
[b] Unpublished data.
[c] Kitamura (2002).

the R_G values for CI and LI together with cyclodextrins and maltooligosaccharides having corresponding DPs. The values for the CIs are smaller than those for the linear ones, indicating that the cyclic chains are more compact. The R_G for CIs are a little bigger (about 0.5 Å) than those for cyclodextrins.

Fig. 5 shows Kratky plots of SAXS experimental data for CIs and LIs. The SAXS profiles of CIs and LIs are very different. CIs with different DPs gave similar scattering profiles, indicating that their shape is similar but the R_G is dependent on the DP. The scattering profiles for LIs have a shape typical of flexible linear chains.

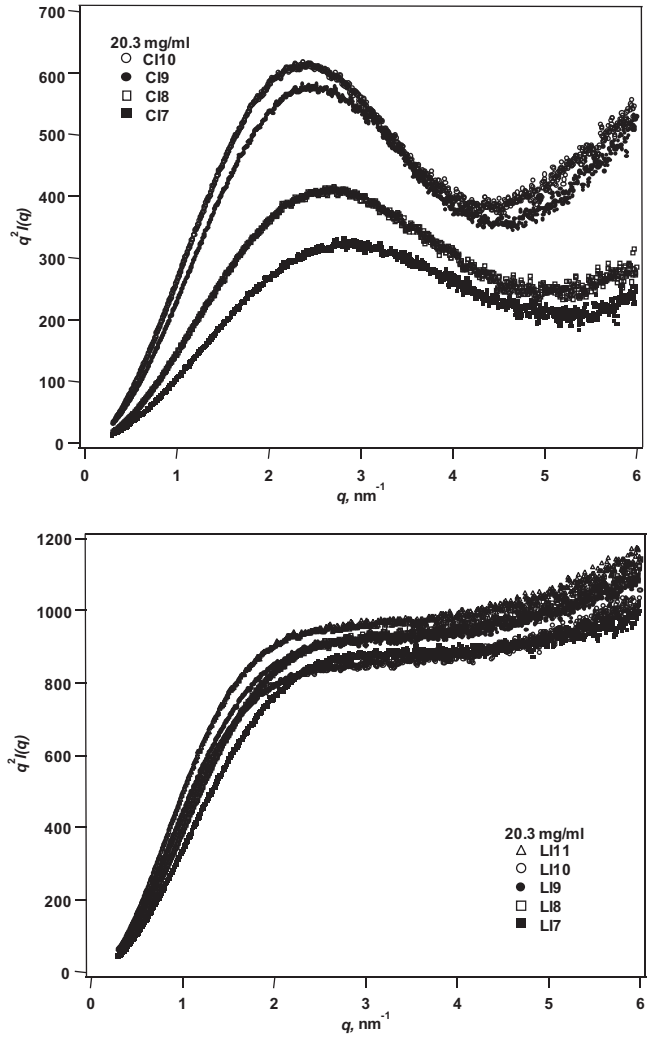

Fig. 5. Kratky plots of SAXS data for four CIs (CI-7, CI-8, CI-9 and CI-10) and five LIs (LI-7, LI-8, LI-9, LI-10 and LI-11).

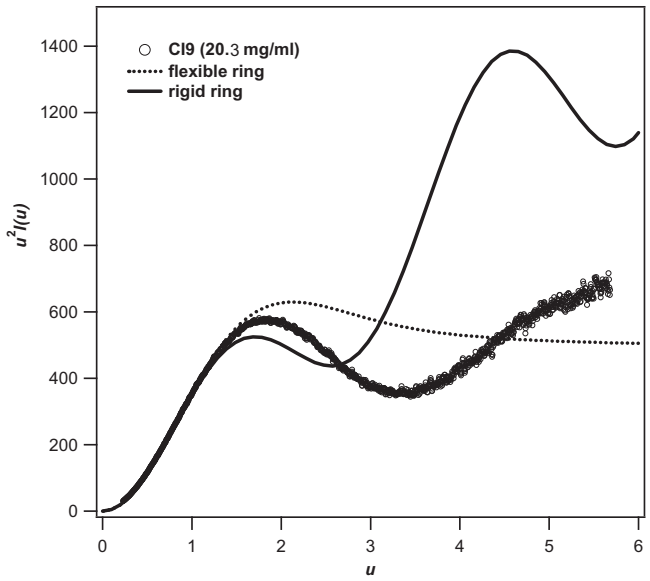

Fig. 6. Kratky plots of SAXS data for CI-9 along with curves calculated for the rigid ring and the flexible ring.

3.4. Molecular modeling and simulation

Fig. 6 compares the experimental SAXS profile of CI-9 with theoretical scattering profiles calculated from two elementary models, a rigid ring (Burchard, 1986) and a flexible Gaussian ring (Burchard & Schmidt, 1980; Casassa, 1965). This comparison suggests that the CI-9 chain is not accurately represented by these rigid and flexible ring models.

The experimental SAXS profile of CI-9 was further compared with theoretical scattering profiles calculated from several models derived from molecular dynamics simulation. Between 1100 and 2300 ns, the R_G value of 395 models fluctuated in the range of 1.0 Å around its mean. We created a histogram of these R_G values with 10 classes at 0.1 Å intervals. It showed a single-peak distribution from 6.1 to 7.1 Å having a peak at the 6.5–6.6 Å class. From each class, we picked out 19 models with lower total energy, so that the frequency distribution of the histogram of these 19 models is similar to that of the full 395. The scattering and average scattering profiles of the 19 models, which are snapshots at 1100, 1208, 1211, 1220, 1337, 1340, 1346, 1352, 1499, 1553, 1745, 1997, 2066, 2078, 2225, 2243, 2246, 2255 and 2258 ns are shown in Fig. 7(a). The scattering profile fluctuates, reflecting a conformational change of the molecule with time. In Fig. 7(a), the experimental data of CI-9 are compared with an additional model **A** (shown in Fig. 7(b)). The scattering profile for the large ring model (model **A**) yields less satisfactory results. The averaged curve for several models is the most satisfactory. Deviation from experimental results at q range higher than 4 has been observed for pullulan oligomers using similar SAXS simulation (Liu et al., 1999). Liu et al. have pointed out that the van der Waals radius when scaled by a factor of 0.6 for C and O atoms showed improved agreement in the high q region.

The flexibility of a glucan chain is mainly the result of rotation about the bonds of the glycosidic linkages, since a pyranose ring is rather rigid. Several results have been reported on conformational analysis of cyclic oligosaccharides, such as cyclosophorose (Mimura et al., 1996) and cyclomaltooligosaccharide with DP 21 (Kitamura, 2002; Kitamura et al., 1997). Whereas in these oligosaccharides the linkage between glucopyranose residues contains two bonds (C-2′, O, C-1 for cyclosophorose and C-4′, O, C-1 for cyclomaltooligosaccharide), in the (1 → 6)-linked glucans the linkage contains three

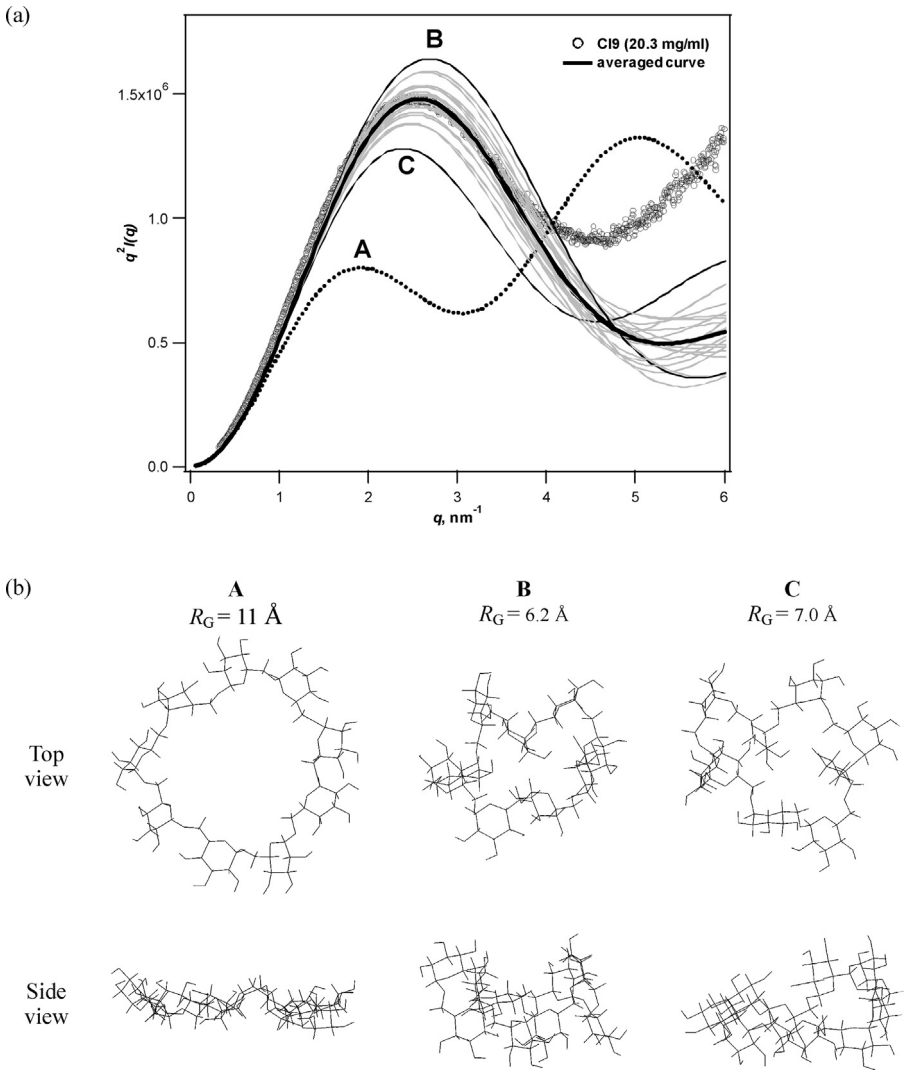

Fig. 7. Kratky plots of SAXS data for CI-9, along with scattering profiles calculated for 19 models from the dynamic model of CI-9 and the average curve of the 19 scattering profiles (a). Model A shown in (b) is a large ring model with an R_G value of 11 Å whose scattering profile is also inserted in (a). Models B and C are models with R_G values of 6.2 Å and 7.0 Å, respectively, which are two of the 19 models used for the calculation (the snapshots at 2243 ns and 1553 ns, respectively).

bonds (C-5′, C-6′, O, C-1). The torsion angles are defined as $\phi = \theta$[O-5, C-1, O, C-6′], $\varphi = \theta$[C-1, O, C-6′, C-5′] and $\omega = \theta$[O, C-6′, C-5′, O-5′]. We analyzed the torsion angles of the 19 models. φ was most likely to fluctuate, so the flexibility of the CI ring is most affected by the torsion angle of φ.

In conclusion, we isolated four cyclic isomaltooligosaccharide samples, CI-7–CI-10, and five linear isomaltooligosaccharide samples, LI-7–LI-11. Using these samples, we studied the conformation and physical properties of cyclic and linear isomaltooligosaccharides in aqueous solution by intrinsic viscosity measurement and SAXS measurement. The values of α in the Mark–Houwink–Sakurada equation for the CI and LI were determined to be 0.50 and 0.78, respectively. The R_G values of CI-7, CI-8, CI-9 and CI-10 determined from SAXS data were 6.7, 6.9, 7.5 and 8.3 Å, respectively. These values are about 0.5 Å larger than those for cyclodextrins with corresponding DPs. To analyze the conformation of CI-9, the Kratky plots of SAXS experimental data for CI-9 were fitted to theoretical scattering profiles calculated using molecular modeling. Results indicate that the CI-9 molecular chain forms a rather compact circular conformation and the R_G for CI-9 fluctuates around its mean. The flexibility of CI-9 may be caused mainly by its α-1,6-glycosidic linkages which contains three bonds (C-5′, C-6′, O, C-1) between each pair of glucose residues. The flexibility of the CI ring might be affected mostly by the torsion angle of φ.

The coordinate data of 3-D structures used in this publication will be made available on request to the corresponding author by CD or e-mail.

Acknowledgments

The synchrotron radiation experiments were performed at the BL40B2 of SPring-8 with the approval of the Japan Synchrotron Radiation Research Institute (JASRI) (Proposal No. 2011B1277 and No. 2012A1261). This work was supported by the Program for Promotion of Basic and Applied Researches for Innovations in Bio-oriented Industry (BRAIN, Japan).

Appendix A.

See Table A.1 and Fig. A.1.

Table A.1
Intrinsic viscosity [η] and Huggins constant k' for CI and LI samples in aqueous solution at 25 °C.

	DP	$[\eta]$ ($cm^3\,g^{-1}$)	$10^3 k'$ ($g\,cm^{-3}$)
CI			
	7	2.92 ± 0.01	0.3 ± 1.0
	8	3.07 ± 0.05	3.9 ± 7.0
	9	3.27 ± 0.01	2.6 ± 3.4
	10	3.48 ± 0.02	4.5 ± 5.6
LI			
	7	3.31 ± 0.01	7.5 ± 0.9
	8	3.64 ± 0.07	5.4 ± 3.6
	9	3.96 ± 0.02	5.4 ± 0.7
	10	4.27 ± 0.01	2.7 ± 0.5
	11	4.69 ± 0.11	−0.3 ± 3.0

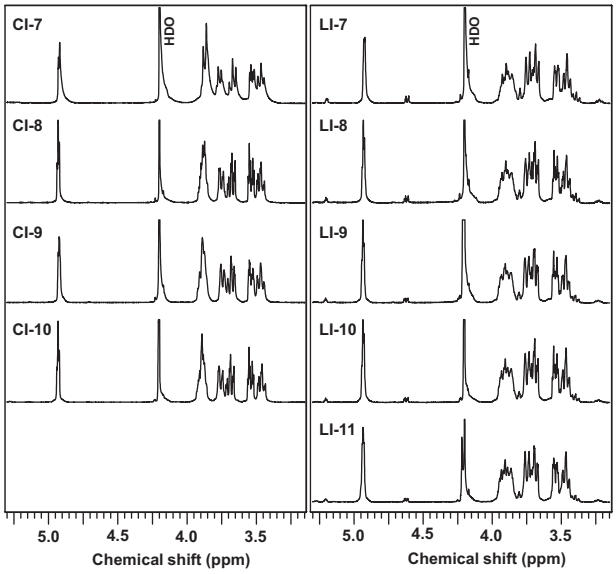

Fig. A.1. ^{1}H NMR spectra of CIs and LIs.

References

Bondi, A. (1964). van der Waals Volumes and Radii. *The Journal of Physical Chemistry*, *68*, 441–451.

Brooks, B. R., Brooks, C. L., 3rd, Mackerell, A. D., Jr., Nilsson, L., Petrella, R. J., Roux, B., et al. (2009). CHARMM: the biomolecular simulation program. *Journal of Computational Chemistry*, *30*, 1545–1614.

Burchard, W. (1986). Theory of cyclic macromolecules. In J. A. Semlyen (Ed.), *Cyclic polymers* (pp. 43–84). London: Elsevier Applied Science Publishers.

Burchard, W., & Schmidt, M. (1980). Static and dynamic structure factors calculated for flexible ring macromolecules. *Polymer*, *21*, 745–749.

Casassa, E. F. (1965). Some statistical properties of flexible ring polymers. *Journal of Polymer Science: Part A: General Papers*, *3*, 605–614.

Funane, K., Terasawa, K., Mizuno, Y., Ono, H., Gibu, S., Tokashiki, T., et al. (2008). Isolation of *Bacillus* and *Paenibacillus* bacterial strains that produce large molecules of cyclic isomaltooligosaccharides. *Bioscience Biotechnology and Biochemistry*, *72*, 3277–3280.

Funane, K., Terasawa, K., Mizuno, Y., Ono, H., Miyagi, T., Gibu, S., et al. (2007). A novel cyclic isomaltooligosaccharide (cycloisomaltodecaose, CI-10) produced by *Bacillus circulans* T-3040 displays remarkable inclusion ability compared with cyclodextrins. *Journal of Biotechnology*, *130*, 188–192.

Gekko, K., & Noguchi, H. (1971). Physicochemical studies of oligodextran. I. Molecular weight dependence of intrinsic viscosity, partial specific compressibility and hydrated water. *Biopolymers*, *10*, 1513–1524.

Glatter, O. (1980). Computation of distance distribution-functions and scattering functions of models for small-angle scattering experiments. *Acta Physica Austriaca*, *52*, 243–256.

Goebel, C. V., Dimpfl, W. L., & Brant, D. A. (1970). The conformational energy of maltose and amylose. *Macromolecules*, *3*, 644–654.

Green, D. F. (2008). Optimized parameters for continuum solvation calculations with carbohydrates. *The Journal of Physical Chemistry B*, *112*, 5238–5249.

Im, W., Lee, M. S., & Brooks, C. L., 3rd. (2003). Generalized born model with a simple smoothing function. *Journal of Computational Chemistry*, *24*, 1691–1702.

Kitamura, S. (2002). Cyclic oligosaccharides and polysaccharides. In J. A. Semlyen (Ed.), *Cyclic Polymers* (pp. 125–160). Dordrecht: Kluwer Academic Publishers.

Kitamura, S., Isuda, H., Shimada, J., Takada, T., Takaha, T., Okada, S., et al. (1997). Conformation of cyclomaltooligosaccharide ("cycloamylose") of dp21 in aqueous solution. *Carbohydrate Research*, *304*, 303–314.

Kobayashi, M., Funane, K., & Oguma, T. (1995). Inhibition of dextran and mutan synthesis by cycloisomaltooligosaccharides. *Bioscience Biotechnology and Biochemistry*, *59*, 1861–1865.

Liu, J. H. Y., Brant, D. A., Kitamura, S., Kajiwara, K., & Mimura, R. (1999). Equilibrium spatial distribution of aqueous pullulan: small-angle X-ray scattering and realistic computer modeling. *Macromolecules*, *32*, 8611–8620.

Maeda, H., Zhu, X., Suzuki, S., Suzuki, K., & Kitamura, S. (2004). Structural characterization and biological activities of an exopolysaccharide kefiran produced by *Lactobacillus kefiranofaciens* WT-2B^T. *Journal of Agricultural and Food Chemistry*, *52*, 5533–5538.

Mimura, M., Kitamura, S., Gotoh, S., Takeo, K., Urakawa, H., & Kajiwara, K. (1996). Conformation of cyclic and linear (1 → 2)-β-D-glucans in aqueous solution. *Carbohydrate Research*, *289*, 25–37.

Mimura, M., Urakawa, H., Kajiwara, K., Kitamura, S., & Takeo, K. (1995). Gelation and its relevance to the function of polysaccharides. *Macromolecular Symposia*, *99*, 43–55.

Oguma, T., Horiuchi, T., & Kobayashi, M. (1993). Novel cyclic dextrins, cycloisomaltooligosaccharides, from *Bacillus* sp. T-3040 Culture. *Bioscience Biotechnology and Biochemistry*, *57*, 1225–1227.

Oguma, T., Tobe, K., & Kobayashi, M. (1994). Purification and properties of a novel enzyme from *Bacillus* spp. T-3040, which catalyzes the conversion of dextran to cyclic isomaltooligosaccharides. *FEBS Letters*, *345*, 135–138.

Porod, G. (1982). In O. Kratky, & O. Glatter (Eds.), *Small angle X-ray scattering* (pp. 17–51). London: Academic Press.

Shimada, J., Kaneko, H., Takada, T., Kitamura, S., & Kajiwara, K. (2000). Conformation of amylose in aqueous solution: small-angle X-ray scattering measurements and simulations. *Journal of Physical Chemistry B*, *104*, 2136–2147.